

The Asteroid Belt— A Computer Simulation

R. F. Mathis*

Abstract

This initial study uses computer simulation to explore the possibility that the asteroid belt observed today resulted from the breakup of a dwarf planet a few thousand years ago. It is assumed that a catastrophic event occurred, and a computer model of the resulting fragmented dwarf planet is developed. The simulation has two parts. First a model of a planet collision is used to provide a starting point. The output file contains the position, velocity, and size of each of more than 16,000 fragments representing an exploded dwarf planet. In the second part of the simulation, each of the fragments is tracked as it propagates under the gravitational influence of the other fragments, the Sun and the planet Jupiter. In this initial study, collisions are not included. The simulation is run out to 15.75 orbit periods of the original dwarf planet or nearly 82 years in 120-second steps. It is shown that a surprising uniformity of the fragments forms around the entire orbit in this short period of time.

Introduction

A current naturalistic explanation for the origin of asteroids claims that asteroids are the debris that did not coalesce into a planet when the solar system was forming about 4.5 billion years ago (4.5 Ga). Modern asteroids are believed to be the result of gravitational accretion, collisions, and the gravitational effects of the planets on the field of debris. This general model forms the basis for most current asteroid studies.

It is interesting that some believe catastrophic collisions are no longer occurring. In a paper by Bottke et al. (2005, p. 111), we read, “Planet formation models suggest the primordial

main belt experienced a short but intense period of collisional evolution shortly after the formation of planetary embryos.” They go on to describe the main asteroid belt as a “living relic.” Of course they are comparing the term “short period” with 4.5 Ga, but this immediately points to the admission that the time to form the asteroid belt is much shorter than its alleged age.

The purpose of this study is to use a computer simulation to explore the possibility that the asteroid belt resulted from the breakup of a planet a few thousand years ago. A natural result of this study ultimately is to gain some insight into the statistics of collisions of the fragments with the planets includ-

* R. F. Mathis, PhD, Murrieta, CA, rfmathis@ix.netcom.com

Accepted for publication August 12, 2013

ing the Earth and the Earth's moon. Since the starting planet in this simulation is smaller than the moon, it will be referred to as a dwarf planet.

Typically, the first question that comes up when discussing this topic is, "What caused the breakup?" The possibilities seem to be either a collision or an explosion. For example, could heating due to accelerated nuclear decay have caused a pressure buildup that resulted in an explosion? For planets that are similar to Earth, the answer is apparently no (Baumgardner, 2012, personal communication). The structure of the Earth is such that there would be no internal buildup of pressure that could lead to an explosion. However, we could postulate that this planet was uniquely created in such a way that it would explode with an unusual internal buildup of heat; of course this is pure speculation. It is not the purpose of this paper to explore the cause of the planet's breakup. Rather the purpose is to determine whether such a breakup that occurred a few thousand years ago could result in the asteroid belt we observe today. The analysis will proceed under the assumption that a catastrophic event, probably a collision, occurred.

The simulation consists of two parts. First, a model of a planet collision is used to provide a starting point. The output is a file containing the position, velocity, and size of each of more than 16,000 fragments. In the second part of the simulation, each of the fragments is tracked as it propagates under the gravitational influence of the other fragments, the Sun and the planet Jupiter. In principle, the state of the fragments can be stored and analyzed at any subsequent time.

In this initial study, collisions are not included but will be added in subsequent studies. The ability to track more than 16,000 individual fragments is enabled by the use of an NVIDIA GPU (graphics processing unit) using the CUDA platform.

Dwarf Planet Model

The first part of this study is to simulate a dwarf planet that has already broken up with the fragments separated far enough that any remaining collisions can be ignored. We lean heavily on the results of a recent paper by Jutzi, Michel, Benz, and Richardson (Jutzi et al., 2009). This paper describes a numerical simulation of asteroid breakups resulting from collisions. Although their focus is on comparing the results of porous and nonporous target materials, the simulation results and methods are useful here. The Jutzi model includes both the fragmentation of the parent body and the gravitational interactions between the fragments. The fragment size distributions they obtained agree well with observed and computed asteroid size distributions. Since they focused on smaller target objects, up to 200 km diameter, it is necessary to extrapolate their results to larger objects for use here (up to 1000 km diameter).

A common quantity used to compare different collision

models is the catastrophic disruption threshold Q_D^* defined as the specific impact energy leading to a largest fragment containing 50% of the original target's mass (e.g., Jutzi et al., 2009, p. 55). The specific impact energy is defined as $Q = 0.5m_p v_p^2 / M_t$ where m_p and v_p are the projectile mass and velocity respectively and M_t is the target mass. This provides a useful point of reference when considering energy, velocity, and mass distributions.

Initial Dwarf Planet Size

The simulation results to date suggest the possibility of a much smaller initial size than might be expected: smaller than the Moon. Hence, it is referred to as a dwarf planet. There are several issues that bear on this, such as the current volume of the asteroids and the current size distribution of the asteroids. It also turns out that an estimate of the number of asteroid collisions with Earth and Earth's moon ultimately should provide insight into the size of the dwarf planet and the dynamics of the breakup. Subsequent studies are expected to address this issue in more detail.

If the initial dwarf planet was much larger, several issues emerge. First, the event must be energetic enough to produce the fragment sizes observed today. If a large number of larger fragments were produced, then many secondary collisions between large fragments would be required. A preliminary look at collision statistics indicates that collisions certainly will occur. However, most collisions will include at least one of the numerous smaller fragments. As the fragment size increases, there are significantly fewer of them and the collision probabilities decrease accordingly. Another issue is that as the volume of material increases, it ultimately must end up as a greater volume of smaller fragments. The number and size of the observed larger fragments is fixed. More initial material can only go into a greater volume of ever-smaller pieces.

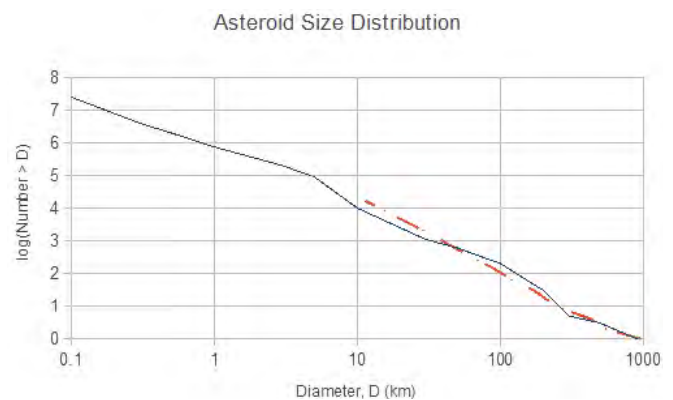


Figure 1. Comparison of simulated asteroid size distribution (dashed line) with published data.

Another issue is the large volume of material from a larger planet. It seems unlikely that a significant fraction of the collision fragments will escape the Sun, or fall into the Sun, even in a much larger, more energetic event. The escape velocity from the Sun at a distance of 3 AU is 24.4 km/s. At 3 AU the dwarf planet is moving at 17.2 km/s and the average fragment velocity is near 3 km/s. The speed distribution is broad enough that some fragments will escape and some will fall into the Sun. However, the smaller fragments tend to have the faster speeds, so the total mass escaping through these means would be relatively small. The average speed increases with dwarf planet size because of the much larger energy required, but this does not appear to be a means for getting rid of a large volume of material.

One interesting possibility for scaling the initial dwarf planet size is that the estimates of numbers of collisions of asteroids with the Earth and the Moon may provide a hook. A particular number density of fragments (fragments per unit volume) intersecting Earth's orbit is directly related to the initial size of the dwarf planet and to the energy of the catastrophic event. In other words the larger the initial dwarf planet, the more fragments will intersect the Earth and Moon.

A lower limit to the size of the original dwarf planet can be obtained using the total mass and average density estimates of the asteroids. In an Asteroid Fact Sheet, NASA estimates the total mass of all of the asteroids as 2.3×10^{21} kg (<http://nssdc.gsfc.nasa.gov/planetary/factsheet/asteroidfact.html>). There are several references that report asteroid mass estimates. One example is labeled "Recent Asteroid Mass Determinations maintained by Jim Baer last updated 12 December 2010." The most recent value for the mass of Ceres is 9.46×10^{20} kg, which differs from NASA's value of 8.7×10^{20} kg. The values given are accompanied by references. In another paper by Krasinsky et al. (2002), it is claimed that estimates prior to that time were too low. Their estimate for the total mass of all the asteroids is $18 \times 10^{10} M \approx 3.6 \times 10^{21}$ kg, which is substantially larger than NASA's value of 2.3×10^{21} kg. Other published values differing from these can be found.

The density of the asteroids varies by the type of material in the asteroid, such as porous, nonporous, rocky core, metallic core, etc. The density used here is 2.1 g/cm^3 , which is the average density of Ceres, the largest asteroid. The mass of Ceres, published by NASA is 8.7×10^{20} kg, which is greater than one-third the estimated mass of all the asteroids combined. Therefore, the density of Ceres was used to approximate the density of all the asteroids. This approximation seems reasonable for a starting point. If necessary it can be refined in future simulations. With these values, the estimated diameter of a dwarf planet comprised of all the known asteroids is 1279 km, or less than 40% the diameter of the Moon (≈ 3476 km). This sets a lower limit to the initial diameter.

Methods

Simulation Fragments

The simulated dwarf planet is assembled using a Monte Carlo approach with a given fragment-size distribution. The resulting equivalent dwarf planet size depends on the number and size of the fragments generated.

The simulation proceeds, first, by assigning a randomly selected radius to each of over 16,000 fragments. There is considerable spread in the published asteroid-size distribution data, but there is a general trend that seems to be common. The data used here (shown in Figure 1) are taken from a paper by Davis et al. (2002). Note that there is a break in the average slope near $D = 5$ km. The average slope for $D > 5$ km is approximately -2.2, while the slope for $D < 5$ km is approximately -1.4. There is a large range in published distributions, and not all of them include this break in the curve. In their collision simulation, Jutzi et al. (2009) obtained a slope of -2.24 for nonporous material and -2.21 for porous material. This is consistent with asteroid formation resulting from collisions.

The simulation includes more than 16,000 fragments. This number with the given distribution restricts the fragment sizes to be greater than 10 km diameter. The dashed curve in Figure 1 shows the final distribution of the fragment sizes used in the simulation. The slope is approximately -2.2. The largest twelve fragments were not selected randomly but instead correspond to the diameters of the published values of the twelve largest asteroids.

The number 16,000 might seem to be too small a number to provide a realistic simulation since Figure 1 indicates that there are tens of millions of asteroids larger than 100 m diameter. Furthermore, extrapolations to even smaller fragments show even larger numbers. However, most of the mass is in the larger asteroids. Estimates depend on assumptions about the distribution, but within this simulation an extrapolation to much larger numbers showed that more than 90% of the total mass is included in the 16,000 largest fragments. This should be treated only as an indication because of the large variations in distribution estimates. However, it points to this being a reasonable starting point for the simulation. The simulated fragments with the above assumptions can be added to get an initial dwarf planet size. This turns out to be 1288 km, which does not include the large number of smaller fragments that would be present in an actual catastrophic event.

Exploded Dwarf Planet Formation. After determining the fragment sizes, the positions of the fragments are uniformly distributed in a unit radius spherical volume. Then each fragment, beginning with the second largest and working to the smallest, is moved radially outward until it is at least a minimum distance from all other fragments. Finally a velocity is assigned

to each fragment. The fragments are modeled as spheres to simplify the code.

The speed distribution of the fragments (Figure 2) is virtually ad hoc with some guidance from papers by Jutzi et al. (2009) and Zappalà et al. (2002). Jutzi et al. (2009) point out that the average, median, and largest ejection speeds scale with target size. They also point out that “smaller fragments tend to have greater ejection speeds than larger ones. However, there is still a wide spread of values for fragments of a given mass, which makes it difficult to define a power-law relationship between fragment masses and speeds” (Jutzi et al., 2009, p. 61). Another constraint in the context of “family-forming events” is discussed by Zappalà et al. (2002). There is a general fit to a model that assumes the maximum kinetic energy is a constant. This results in a power-law trend for the maximum fragment speed as a function of size.

The starting point for determining fragment speeds was an estimate of the size of the original dwarf planet. Then an average speed was obtained by extrapolating the results in Figure 10 of Jutzi et al. (2009). Starting with a modified Rayleigh distribution and adding the maximum speed power-law constraint while maintaining the desired average speed resulted in the distribution shown in Figure 2. The initial direction of each fragment is radially outward from the center of the dwarf planet in the dwarf planet’s reference frame.

Energy considerations can be used for an approximate consistency check. Extrapolating the results of Jutzi et al. (2009) for a nonporous dwarf planet with an impact speed and angle of 3 km/sec and 45° respectively, the value of Q_D^0 is approximately 2.4×10^{10} erg/gm. Compared with the simulation results, the total fragment energy in the simulation is less than 10% of the initial projectile energy. These numbers are very approximate but provide a consistency check.

Figure 3 shows the exploded dwarf planet used as the starting point for the simulation. The randomly assigned colors help to visualize the fragments. Table 1 summarizes the initial parameters.

Fragment Tracking

The second part of the simulation, in which each fragment is tracked in time and space, requires solving the N-Body problem: the problem of predicting the motion of a group of objects that are connected gravitationally. The problem has no closed analytical solution. Here we use a simulation described as an All-Pairs N-Body Simulation. It generally follows the methods described by Nyland et al. (2007). This approach is brute force and relatively simple but is not generally used because of its $O(N^2)$ computational complexity. The use of a GPU with its massively parallel structure is well matched to this problem and provides substantial acceleration in computing speed.

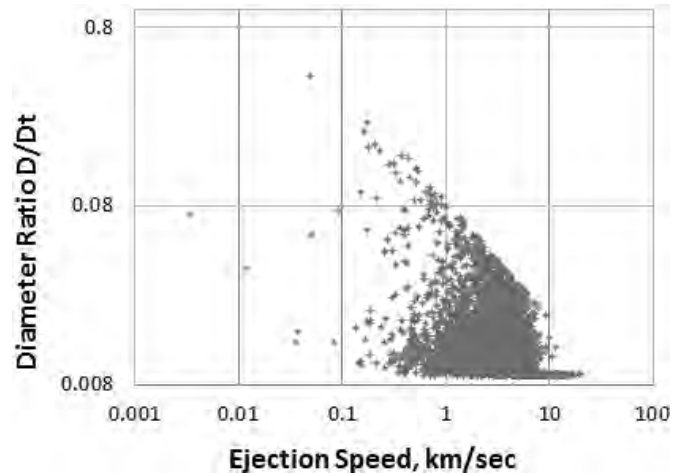


Figure 2. Exploded dwarf planet fragment diameters vs. ejection speed. Dt is initial dwarf planet diameter assuming only these fragments.

The starting point is the array of fragments from the exploded dwarf planet model. Each of the N fragments has three position coordinates, three velocity components, and a fragment radius. As stated above, the fragment densities are assumed constant and equal to the density of the largest asteroid. Therefore each fragment radius can be used to determine each fragment mass. The coordinates and velocities are first transformed from the dwarf planet coordinate system to the solar coordinate system. Then the leapfrog integration method is used to numerically integrate the gravitational differential equations.

Leapfrog integration is a simple, second-order method that conserves energy. The position vector of the i^{th} fragment at time t is given by

$$\vec{x}(t)_i = \vec{x}(t - \Delta t)_i + \vec{v}(t - 0.5\Delta t)_i \cdot \Delta t$$

where $i = 1, \dots, N$, N is the number of fragments, and Δt is the time step. The corresponding acceleration vector is given by

$$\vec{a}(t)_i = \sum_{(1 \leq j \leq N, j \neq i)} \frac{G \cdot m_j \cdot \vec{r}(t)_{ij}}{(r(t)_{ij})^3}$$

in which G is the gravitational constant, m_j is the mass of the j^{th} fragment, and

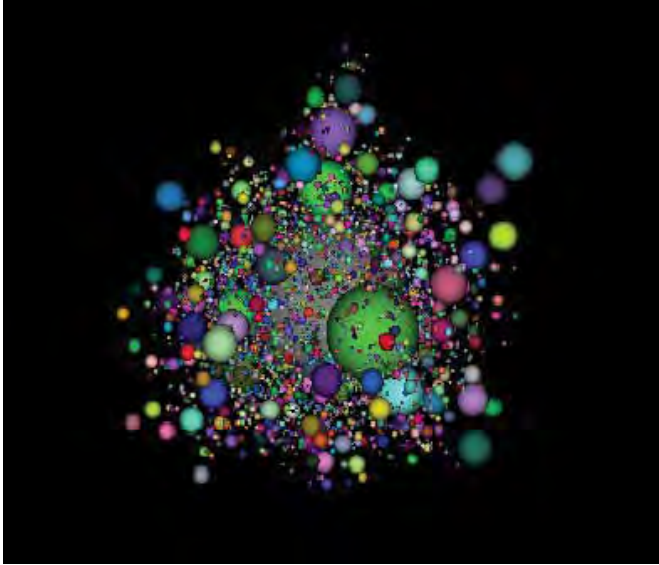


Figure 3. Typical exploded dwarf planet used as a starting point for the simulation. The mean diameter of the swarm of particles shown here is approximately 2,500 km. The randomly assigned colors help to visualize the fragments. Not all fragments are plotted.

$$\vec{r}(t)_{ij} = \vec{x}(t)_j - \vec{x}(t)_i$$

is the vector from fragment i to fragment j . Finally the velocity update of the i^{th} fragment is given by

$$\vec{v}(t + 0.5 \Delta t)_i = \vec{v}(t - 0.5 \Delta t)_i + \vec{a}(t)_i \Delta t$$

Leapfrog integration updates position and velocity at interleaved time points in such a way that they leapfrog over each other. Note that the position and velocity updates require only $O(N)$ computations, while each acceleration update requires $N-1$ computations resulting in $O(N^2)$ computations overall. The GPU processor is used to perform the acceleration update. The GPU approach generally follows that described by Nyland et al. (2007); however, some simplifications were incorporated. The details of the code are not included here. The use of loop unrolling was implemented to increase efficiency. An independent acceleration computation was also implemented using the CPU (Intel i7 processor) and used to verify that the GPU computations were working correctly. It was found that the use of the GPU increased processing speed by a factor of approximately 300 over the use of a single CPU. A newer GPU (Microway's Tesla GPU accelerated cluster) was made

Table 1. Initial Dwarf Planet Parameters Used in Simulation

Number of fragments in dwarf planet	16,383
Fragment mass density (constant for all fragments)	2.1×10^{-3} kg/cm ³
Total mass of fragments	2.35×10^{21} kg
Total fragment energy	1.10×10^{34} erg
Specific fragment energy	4.69×10^9 erg/g
Average speed of fragments	3.24 km/sec
Equivalent (unexploded) diameter	1288 km
Escape velocity from initial dwarf planet surface	0.70 km/sec
Largest fragment diameter	952 km
Initial minimum distance between fragments	100 km

Table 2. Fragment Tracking Details Used in Simulation

Simulation step size	120 sec.
Dwarf planet solar distance (circular orbit)	3 AU
Dwarf planet speed	17.244 km/sec
Dwarf planet period	5.182 years
Jupiter starting point (Arbitrary angle ahead of dwarf planet)	0.75 pi
Jupiter solar distance (Circular orbit, no inclination)	5.203 AU
Jupiter speed	13.06 km/sec
Jupiter period	11.86 years
Escape velocity from Sun at 3 AU (Ignoring the dwarf planet)	24.4 km/sec

available on a trial basis and used to run the simulation out to 15.75 orbits, corresponding to more than 81 years in 120-second steps. (The accelerated computations were performed on Microway's Tesla GPU accelerated compute cluster. The computing speed was increased by more than a factor of three over the use of the original GPU.)

Simulation key parameters are included in Table 2. The objects in the simulation included the dwarf planet fragments, the Sun, and the planet Jupiter. Jupiter was included because it has the largest planetary influence on the asteroids. The position of Jupiter at the starting point was arbitrarily set at 0.75π ahead of the dwarf planet. No orbital inclination was added. Future simulations may include additional planets.

The step size Δt was set at 120 seconds. There are no requirements for high precision, as in satellite trajectory calculations, and no rapid changes in velocity that would require much smaller step sizes. With an average speed in the solar reference frame of greater than 17 km/sec fragments move about 2000 km between steps. With this step size, the Microway Tesla accelerated computer cluster took more than 52 hours of run time to go from 5 to 15 dwarf planet orbits (5.18 years/orbit).

Results

Tracking

Figures 4a through 4f illustrate the results. Note that in order to see the fragments, the plotted diameters were multiplied by

a factor of 20,000. Also the Sun was multiplied by a factor of 12 and Jupiter by a factor of 100. These factors were applied only for visualizing the results of the simulation. Figure 4a illustrates the starting positions. The figure is the x-y plane of a three-dimensional volume. The Sun is at the origin, and the exploding dwarf planet is on the positive x-axis. The planet Jupiter, also shown, is arbitrarily set 0.75π radians ahead of the exploding dwarf planet. The orbits of the inner planets also are indicated, but the planets are not shown.

Initially the fragments spread radially as expected. However, in less than one fourth of an orbit, the pattern of fragments begins to show an elongation (Figure 4b). The elongation is much more evident in Figure 4c. The slower fragments have smaller orbits with shorter periods, while the faster fragments have larger orbits with longer periods. This is further enhanced by the acceleration of the smaller orbit fragments as their radius decreases, while the larger orbit fragments slow as their radius increases. The elongation increases to the point that at the end of a single orbit, there is the appearance of what can be described as filaments (Figure 4d). By the end of 2.5 orbits, the entire orbit of the original dwarf planet is populated with fragments (Figure 4e).

Figure 4f shows the fragments after 15.75 orbits (81.67 years). The differential velocities of the fragments have filled in the distribution of fragments such that it is beginning to approach uniformity around the entire orbit. The obvious exception is the initial collision point to which all fragments return. The only modifying effect included in this simula-

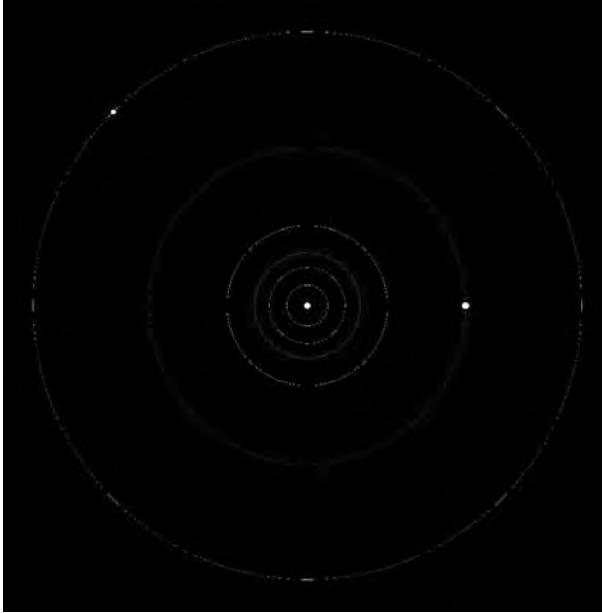


Figure 4a. The figure shows the starting point with the Sun, Jupiter, and the orbits of the inner planets (inner planets are not shown). Visualization is enhanced by artificially increasing the sizes. The Sun's diameter was multiplied by 12; Jupiter's diameter was multiplied by 100, and the asteroid fragment diameters were multiplied by 20,000. Further magnification of the initial dwarf planet would reveal an image similar to Figure 3.

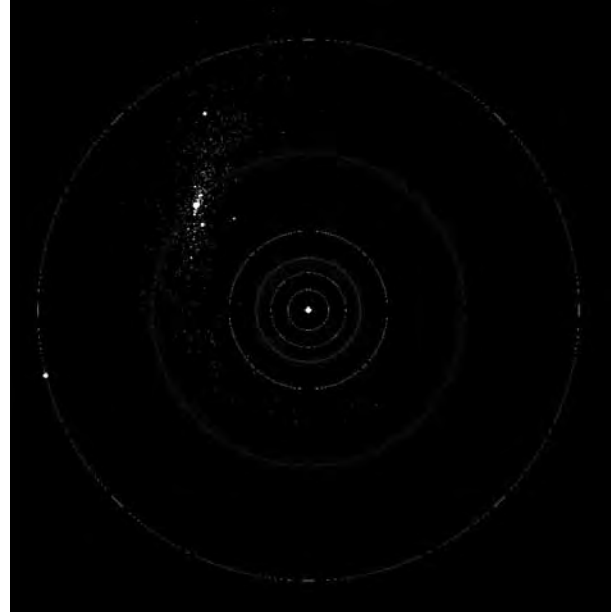


Figure 4c. Asteroid fragments at 0.375 of an orbit of the original dwarf planet (angle is 0.75π radians) corresponding to 1.94 years. The elongation is obvious at this point.

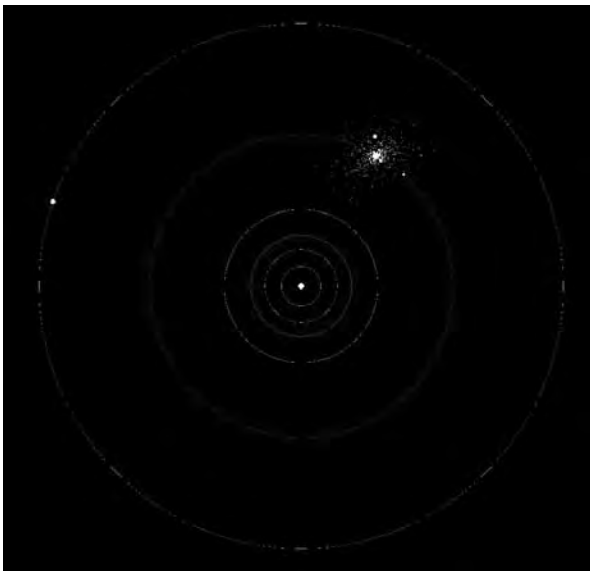


Figure 4b. Asteroid fragments at 0.168 of an orbit of the original dwarf planet (angle is $\pi/3$ radians) corresponding to 0.83 years. An elongation of the pattern is beginning to be apparent.

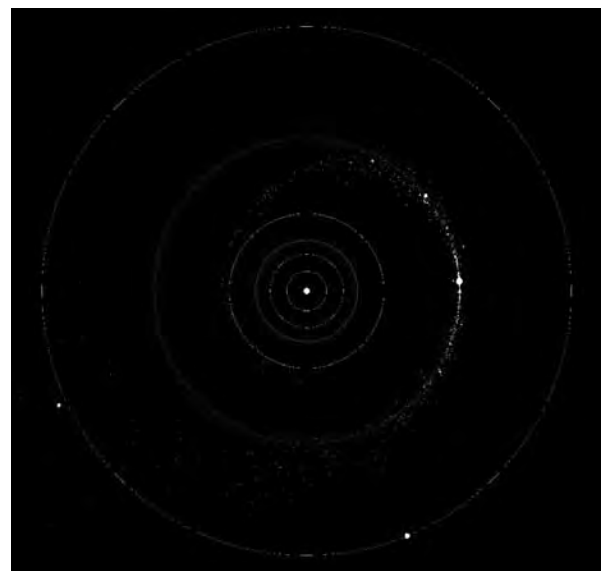


Figure 4d. Asteroid fragments at 1 orbit of the original dwarf planet (angle is 2π radians) corresponding to 5.18 years. Each fragment has an elliptical orbit that returns to the initial collision point. The slower fragments with smaller orbits and shorter periods get ahead of the faster fragments with larger orbits and longer periods, giving the appearance of filaments.

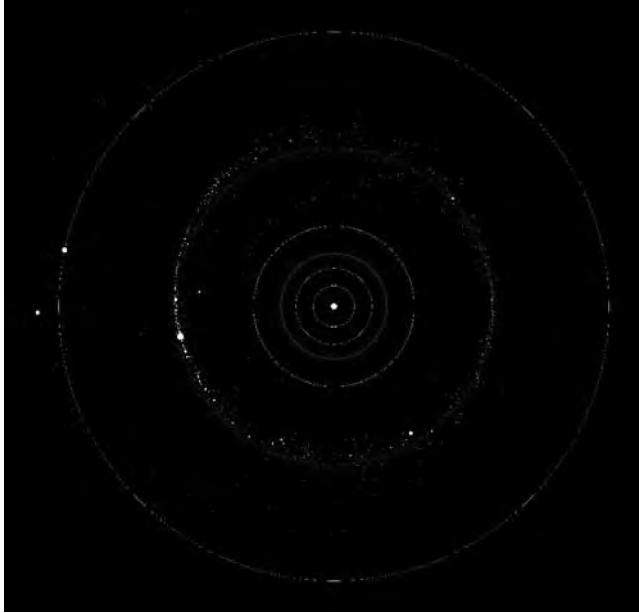


Figure 4e. Asteroid fragments at 2.5 orbits of the original dwarf planet (angle is 5π radians) corresponding to 12.96 years. The remains of the initial filaments are still evident. The entire orbit of the original dwarf planet is populated with fragments. Again all fragments return to the original collision point.

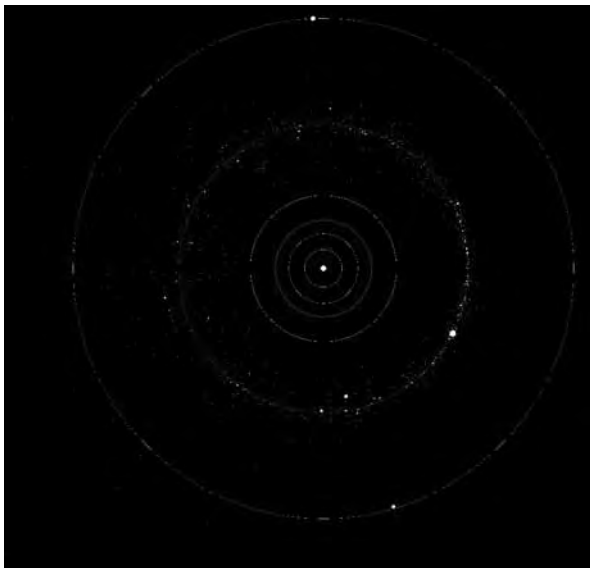


Figure 4f. Asteroid fragments at 15.75 orbits of the original dwarf planet (angle is 31.5π radians) corresponding to 81.67 years. At this point the density of fragments around the entire orbit is becoming more uniform. Clearly, collisions are required to eliminate the return of all orbits to the collision point.

tion is the effect of the planet Jupiter, which can be expected to perturb a few of the fragments. Note that Jupiter orbits only 6.9 times in this initial 81.67 years. The obvious missing effect is that of collisions, which were not included.

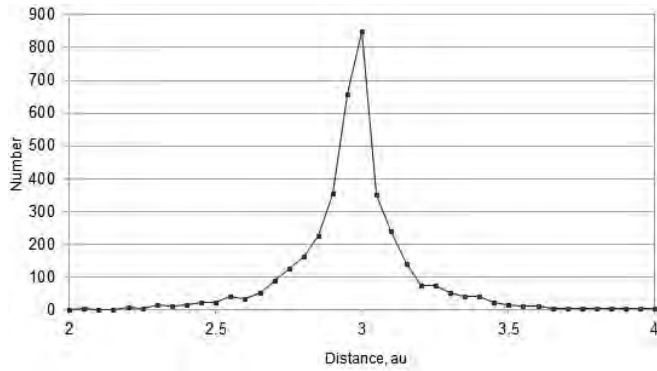
It is remarkable how quickly the fragments are becoming uniformly distributed. This is illustrated in Figures 5a–5d, which plot the density of fragments with distance from the Sun after 15.75 orbits at four different positions, centered at 0° , 90° , 180° , and 270° , including all fragments within $\pm 45^\circ$ at each position. At 0° the distribution is narrower as expected, since all of the fragments return to the collision point. A combination of collisions and perturbations from the other planets ultimately will spread out this section. The other directions (Figures 5b–5d) show distributions with similar widths and heights. In the position opposite the collision point (Figure 5c), there are peaks that may be remnants of the initial filaments, although they are not seen in the other directions. The number of fragments in each of these directions is also remarkably similar. In order they are 4038 at 0° , 3658 at 90° , 4575 at 180° , and 4112 at 270° . Overall about 10% are at very large distances, with most of the large-distance fragments skewed toward the 180° direction as expected.

Figures 5b–5d do not show any signs of Kirkwood gaps. Kirkwood gaps are gaps in the radial distribution, presumably due to orbital resonances between the fragment periods and the period of the planet Jupiter. The fact that they are not seen is not surprising since 15.75 orbits of the dwarf planet collision point corresponds to only 6.9 orbits of Jupiter as mentioned earlier.

Collisions

A preliminary look at collisions verified that they are virtually certain. As fragments approach the original collision point, they necessarily increase their density and therefore collision probability. Furthermore, different fragments return to this point at different times with different velocities, providing a substantial relative velocity between colliding fragments. Figure 6 illustrates the velocity distribution at the collision point after 1.5 orbits of the collided dwarf planet. Since all unperturbed fragments must return to this point, a relatively broad speed distribution results, which increases the probability of collisions. There are several observations to be made concerning collisions.

1. Collision probabilities will significantly increase with decreasing fragment size. As stated earlier, this simulation includes only the 16,000 largest fragments (diameters of 10 km and larger). There are at least 1000 smaller fragments (100 m diameter or greater) for each fragment in this simulation. The presence of even greater numbers of even smaller fragments is estimated in some studies.
2. The probability of collisions between larger fragments decreases rapidly with increase in size. This implies that it is very unlikely that the starting point is a much larger



Figures 5a–5d. These figures show the distribution of fragments in each of four directions after 15.75 orbits after the collision. Figures 5a through 5d correspond in order to 0° , 90° , 180° , and 270° . Each figure includes the fragments from $\pm 45^\circ$ around the given direction. The distribution in Figure 5a is narrower than the others because it includes the collision point. It is remarkable that the fragments are this uniform after only 82 years. The orbit of the initial dwarf planet had a radius of 3 AU.

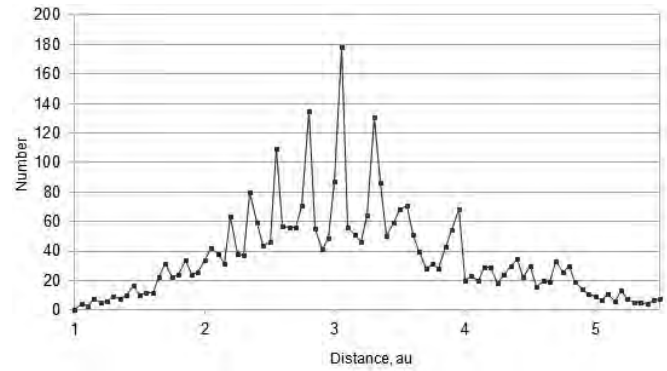


Figure 5c. The distribution at $180^\circ \pm 45^\circ$ is broader than the others and has pronounced peaks. The peaks may be the remnants of the filaments seen in Figures 4d and 4e.

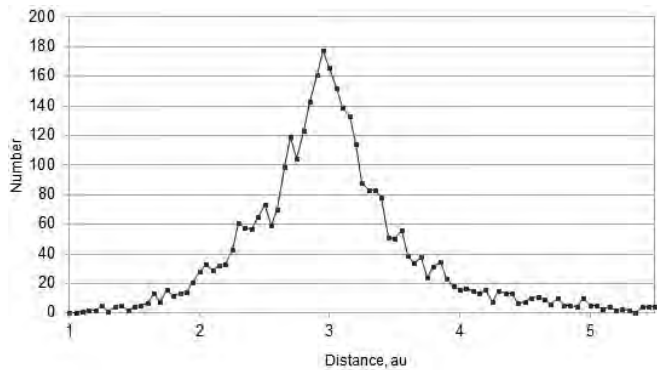


Figure 5b. The distribution of fragments in the $90^\circ \pm 45^\circ$ direction.

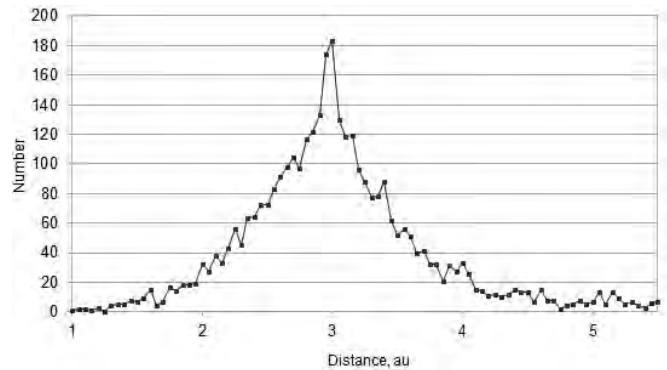


Figure 5d. The distribution of fragments in the $270^\circ \pm 45^\circ$ direction.

planet with many large fragments that collide, producing the smaller fragments observed today. Some collisions between the larger fragments can be expected, but they will be much less likely.

- There are a number of papers on the existence of asteroid families, defined as groups of asteroids with common characteristics that presumably resulted from catastrophic collisions early in the formation of the solar system (cf. Bendjoya and Zappalà, 2002). This provides another motivation for developing a simulation that includes collisions.

Summary

A computer simulation was used to explore the possibility that the asteroid belt could form in a few thousand years as the result of a catastrophic breakup of a dwarf planet. First, a computer model of an exploding dwarf planet was developed based on the results of recent asteroid collision studies. The result was a file containing the position, velocity, and size of each of more than 16,000 explosion fragments. Then each of the fragments was tracked as it propagated under the gravitational influence of the other fragments, the Sun, and the planet Jupiter. An

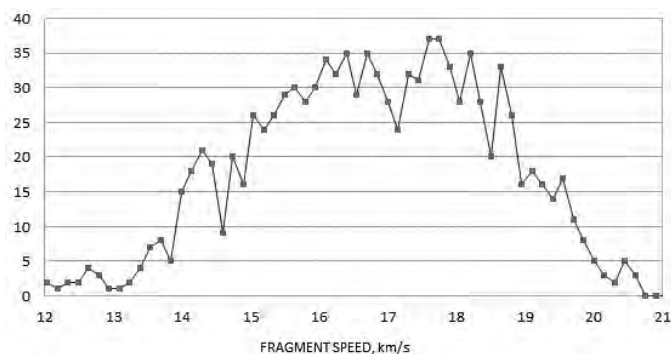


Figure 6. Speed distribution of fragments near collision point after 1.5 orbits of the collided dwarf planet. All unperturbed fragments must return through this point, resulting in large relative velocities.

All-Pairs N-Body Simulation approach is used with a Leapfrog integration algorithm. This brute-force approach was enabled by the use of a GPU using the CUDA platform. The simulation was carried out to 15.75 orbits of the collided dwarf planet, or nearly 82 years in 120-second steps.

These initial results showed that a relatively uniform distribution of fragments formed around the entire orbit of the original dwarf planet in this surprisingly short time. Since each fragment is in essentially a constant elliptic orbit unless perturbed, they almost all return to the collision point. This means that either collisions or perturbations from the other planets are required for complete uniformity. A preliminary analysis showed that collisions are virtually certain, especially during the first few orbits.

The results are consistent with the formation of the observed asteroid belt in a few thousand years. However, the study is certainly not complete. Many questions remain. For example, how long will it take to see the formation of the observed radial distribution including the Kirkwood gaps? And, can a

simulation such as this show the formation of Greeks, Trojans, and Hildas, objects assumed to be asteroids orbiting close to the conjugate points of Jupiter? A great deal of work remains.

Acknowledgments

I thank God for an opportunity and the enabling to explore a tiny part of His amazing creation. I would like to thank Don DeYoung, who initially proposed this project, for helpful discussions along the way. I would like to thank John Baumgardner and Steve Austin for helpful discussions as well, and I would like to thank my son, David Mathis, for his expert help with programing details and the subtleties of Linux.

References

- Bendjoya, Ph. and V. Zappalà. 2002. Asteroid family identification. In Bottke, W.F. Jr., A Cellino, P. Paolicchi, and R.P. Binzel (editors), *Asteroids III*, pp. 613–618. University of Arizona Press, Tucson, AZ.
- Bottke, W.F. Jr., D.D. Durda, D. Nesvorný, R. Jedicke, A. Morbidelli, D. Vokrouhlický, and H. Levison. 2005. The fossilized size distribution of the main asteroid belt. *Icarus* 175:111–140.
- Davis, Donald R., Daniel D. Durda, Francesco Marzari, Adriano Campo Bagatin, and Ricardo Gil-Hutton. 2002. Collisional evolution of small-body populations. In Bottke, W.F. Jr., A Cellino, P. Paolicchi, and R.P. Binzel (editors), *Asteroids III*, pp. 545–558. University of Arizona Press, Tucson, AZ.
- Jutzi, Martin, Patrick Michel, Willy Benz, and Derek C. Richardson. 2009. Fragment properties at the catastrophic disruption threshold: the effect of the parent body's internal structure. *Icarus* 207:54–65.
- Krasinsky, G.A., E.V. Pitjeva, M.V. Vasilyev, and E.I. Yagudina. 2002. Hidden mass in the asteroid belt. *Icarus* 158:98–105.
- Nyland, Lars, Mark Harris, and Jan Prins. 2008. Fast N-body simulation with CUDA. In Nguyen, Hubert (editor), *GPU Gems 3*, pp. 677–695. NVIDIA Corporation, Boston, MA.
- Zappalà, V., A. Cellino, A. Dell'Oro, and P. Paolicchi. 2002. Physical and Dynamical Properties of Asteroid Families. In Bottke, W.F. Jr., A Cellino, P. Paolicchi, and R.P. Binzel (editors), *Asteroids III*, pp. 619–631. University of Arizona Press, Tucson, AZ.